nutrition and health. *LeMADS-RIN* represents a molecular bridge between the extensively studied phenomena of floral development and fruit ripening/ethylene response with regard to the cascade of ethylene-regulated events associated with climacteric ripening being dependent on a member of the floral development–associated MADS-box family. This discovery opens a new research frontier in fruit ripening. For example, because MADS-box genes are known to act as multimers (*26*), one could logically predict that additional MADS-box genes might affect ripening.

From a practical perspective, the *rin* mutation is widely used in tomato hybrid cultivars to yield fruit with a long shelf life and acceptable quality. Tomatoes heterozygous for the *rin* allele remain firm and ripen over a protracted period (presumably due to reduced levels of functional RIN protein) permitting industrial-scale handling and expanded delivery and storage opportunities. *LeMADS-RIN* is a rare example of a gene whose effects are documented a priori, suggesting excellent potential for practical genetic modification of fruit ripening and quality characteristics.

**References and Notes**


1. M. Rhodes, in *Senescence in Plants*, K. V. Thimann, Ed., (CRC, Boca Raton, 1980), pp. 157–205.
2. G. Seymour, J. Taylor, G. Tucker Eds., *Biochemistry of Fruit Ripening* (Chapman & Hall, London, 1993).
3. J. Giovannoni, *Annu. Rev. Plant Physiol. Plant Mol. Biol.* **52**, 725 (2001).
4. Tomato molecular and genetic resources can be found online through the Solanaceae Genomics Network (http://www.sgn.cornell.edu/) and TIGR Tomato Gene Index (http://www.tigr.org/tdb/lgi/).
5. J. Fillatti, J. Kiser, B. Rose, L. Comai, in *Tomato Biotechnology*, D. Nevins, R. Jones, Eds. (Liss, New York, 1987), pp. 199–210.
6. E. Tigchelaar, W. McGlasson, R. Buescher, *Hort. Sci.* **13**, 508 (1978).
7. H. Yen *et al.*, *Plant Physiol.* **107**, 1343 (1995).
8. J. Lincoln, R. Fischer, *Plant Physiol.* **88**, 370 (1988).
9. J. Giovannoni *et al.*, *Mol. Gen. Genet.* **248**, 195 (1995).
10. M. Ng, M. Yanofsky, *Nature Rev. Genet.* **2**, 186 (2001).
11. G. Theissen, *Curr. Opin. Plant Biol.* **4**, 75 (2001).
12. R. Robinson, M. Tomes, *Rep. Tomato Genet. Coop.* **18**, 36 (1968).
13. Details of Yrin9 mapping, cDNA isolation, plant transformation constructs, and phylogenetic analysis can be found on *Science* Online at www.sciencemag.org/cgi/content/full/296/5566/343/DC1.
14. C34 (*LeMADS-MC*) primers are C34F 5′GAAGATGGGAAGAGGAAAAGTTGAATTAAGA3′ and C34R 5′GGTTCTATACATGCATATCAATATAAAGACACTCAA3′. C43 (*LeMADS-RIN*) primers are C43F 5′GACGGGAACCATTAGATTTTAAAGACA3′ and C43R 5′GTGTTATCAATATTGCCATACTCTTCTTGACAA3′.
15. GenBank accession numbers are C34 (LeMADS-MC), AF448521; C43 (LeMADS-RIN), AF448522; and C43/34 (*rin* mutant), AF448523.
16. Primers were designed to amplify the region separating the C34 and C43 transcribed regions, as shown in Fig. 3C. The primers used were designated as G34R 5′TCTTAATTCAACTTTTCCTCTTCCCATCTTC3′ and G43F 5′TTGTCAAGAAGAGTATGGCAATATTGATAACAC3′.
17. G. Theissen, J. Kim, H. Saedler, *J. Mol. Evol.* **43**, 484 (1996).
18. J. Reichmann, E. Meyerowitz, *Biol. Chem.* **378**, 1079 (1997).
19. E. Alvarez-Buylla *et al.*, *Plant J.* **24**, 457 (2000).
20. L. Pnueli, D. Hareven, S. D. Rounsley, M. Yanofsky, E. Lifschitz, *Plant Cell* **6**, 163 (1994).
21. C. Gustafson, B. Savidge, M. F. Yanofsky, *Cell* **76** 131 (1994).
22. P. Huijser *et al.*, *EMBO J.* **11**, 1239 (1992).
23. S. Pelaz, G. Ditta, E. Baumann, E. Wisman, M. Yanofsky, *Nature* **405**, 200 (2000).
24. H. Huang, M. Tudor, T. Su, Y. Hu, H. Ma, *Plant Mol. Biol.* **28**, 549 (1995).
25. J. Vrebalov, D. Medrano, J. Giovannoni, unpublished data.
26. J. Reichmann, B. Krizek, E. Meyerowitz, *Proc. Natl. Acad. Sci. U.S.A.* **93**, 4793 (1996).



27. We thank S. Tanksley for restriction fragment length poymorphism markers, the tomato YAC library, and intellectual support throughout this project; G. Seymour and K. Manning for the strawberry fruit cDNA library; and M. Yanofsky, H. Klee, and C. Barry for helpful discussions. Supported by the Texas Agricultural Experiment Station, USDA-NRI grants 92-37300-7653 and 95-37300-1575, NSF grants IBN-9604115 and DBI-9872617, and Zeneca Agrochemicals.

19 November 2001; accepted 2 February 2002


# Alteration of Lymphocyte Trafficking by Sphingosine-1-Phosphate Receptor Agonists


**Suzanne Mandala,[1] Richard Hajdu,[1] James Bergstrom,[1] Elizabeth Quackenbush,[2] Jenny Xie,[2] James Milligan,[1] Rosemary Thornton,[1] Gan-Ju Shei,[1] Deborah Card,[1] CarolAnn Keohane,[1] Mark Rosenbach,[1] Jeffrey Hale,[3] Christopher L. Lynch,[3] Kathleen Rupprecht,[3] William Parsons,[3] Hugh Rosen[1]***



**Blood lymphocyte numbers, essential for the development of efficient immune responses, are maintained by recirculation through secondary lymphoid organs. We show that lymphocyte trafficking is altered by the lysophospholipid sphingosine-1-phosphate (S1P) and by a phosphoryl metabolite of the immunosuppressive agent FTY720. Both species were high-affinity agonists of at least four of the five S1P receptors. These agonists produce lymphopenia in blood and thoracic duct lymph by sequestration of lymphocytes in lymph nodes, but not spleen. S1P receptor agonists induced emptying of lymphoid sinuses by retention of lymphocytes on the abluminal side of sinus-lining endothelium and inhibition of egress into lymph. Inhibition of lymphocyte recirculation by activation of S1P receptors may result in therapeutically useful immunosuppression.**


T and B lymphocytes migrate from their sites of lymphopoiesis (thymus and bone marrow), traverse the blood stream, and enter the appropriate secondary lymphoid organ (SLO) where they may either enter a specialized compartment to await antigen, or egress from lymph nodes (*1*). Egressing lymphocytes cross an endothelial barrier from the ablumi-

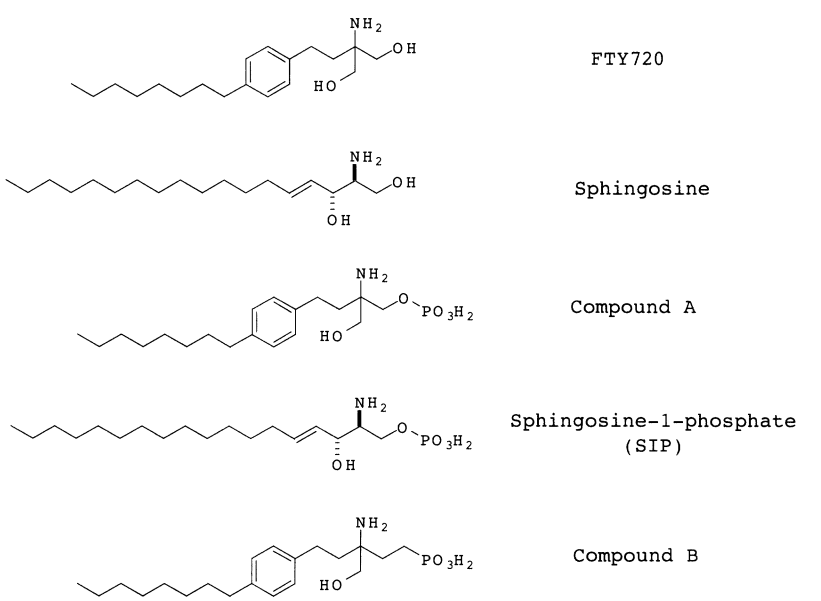


**Fig. 1.** The structures of FTY720, S1P and related synthetic compounds.

nal side to enter the efferent lymphatics, eventually returning to the blood stream through the thoracic duct, and thus recirculate. Like naïve T cells, long-lived central memory T cells follow this constitutive homing and recirculation paradigm, whereas effector cells may also leave blood through postcapillary venules and return to SLO through afferent lymph (*2*).

The signals governing lymphocyte homing and retention in B and T cell areas of SLO that have been elucidated include selectin-mediated cell rolling, integrin-dependent transendothelial migration, spatially regulated expression, and activation of counter-receptors, chemokines, and their cognate G protein–coupled receptors such as CCR7 and CXCR5 (*3*). In contrast, the molecular basis of the regulated maintenance of circulating lymphocyte levels in peripheral blood, and within the recirculation pathway has been slower in emerging. In a reverse pharmacological experimental approach, we have clarified the mechanism of action of an immunosuppressive agent, FTY720, known to sequester lymphocytes in SLO (*4*), and defined the role of the biologically active lysophospholipid sphingosine-1-phosphate (S1P), as a potent agonist that regulates the lymphocyte recirculation pathway.

Although FTY720 appears to cause immunosuppression by sequestration of lymphocytes in SLO (*5*), its mechanism of action has not been clear. It has been described as having no biologically active metabolites (*4, 6*). However, it shares structural homology to the lysophospholipid sphingosine (Fig. 1). We therefore postulated that it was a sphingosine analog, and a potential substrate for, or an inhibitor of, sphingosine-metabolizing enzymes. Pharmacokinetic analysis of FTY720 by liquid chromatography mass spectrometry (LC-MS) (*7*) in mice and rats revealed an additional molecular species of +80 atomic mass units (Fig. 2). After compound administration in vivo, this metabolite was in equilibrium with the parent compound, and was the dominant molecular species in rat plasma. The metabolite was also produced upon incubation of [$^3$H]-labeled FTY720 with blood from rat, chicken, dog, rhesus macaque, and man (*8*). When synthesized biochemically by incubation of FTY720 in rat blood and purified to homogeneity, the structure was confirmed by nuclear magnetic resonance analysis to be the phosphate ester metabolite of FTY720 (Compound A), a close structural homolog of S1P (Fig. 1). Incubation of lymph node–derived cells, as well as COS, CHO, and HEK cells, with FTY720 readily produced Compound A in vitro (*8*). Neither FTY720 nor Compound A were inhibitors of serine palmitoyltransferase activity catalyzed by LCB1/LCB2 (*9*), nor were they inhibitors of sphingolipid biosynthesis or metabolism (*8*).

We postulated that Compound A was an agonist ligand of lysophospholipid receptors for S1P. G protein–coupled receptors for S1P (*10–12*) are expressed both on endothelial cells ($S1P_1$, $S1P_3$), and mRNA can be detected in lymphoid tissues [$S1P_1$ (edg1), $S1P_2$ (edg5), $S1P_3$ (edg3), $S1P_4$ (edg6), $S1P_5$ (edg8)] (*13*). The activity of synthetic Compound A (*7*) was evaluated in a radioligand competitive binding assay using [$^{33}$P]-labeled S1P ($S1^{33}P$) on transfected CHO cells ex-

Departments of [1]Immunology and Rheumatology, [2]Pharmacology, and [3]Medicinal Chemistry, Merck Research Laboratories, Post Office Box 2000, Rahway, NJ 07065, USA.

*To whom correspondence should be addressed. E-mail: hugh_rosen@merck.com

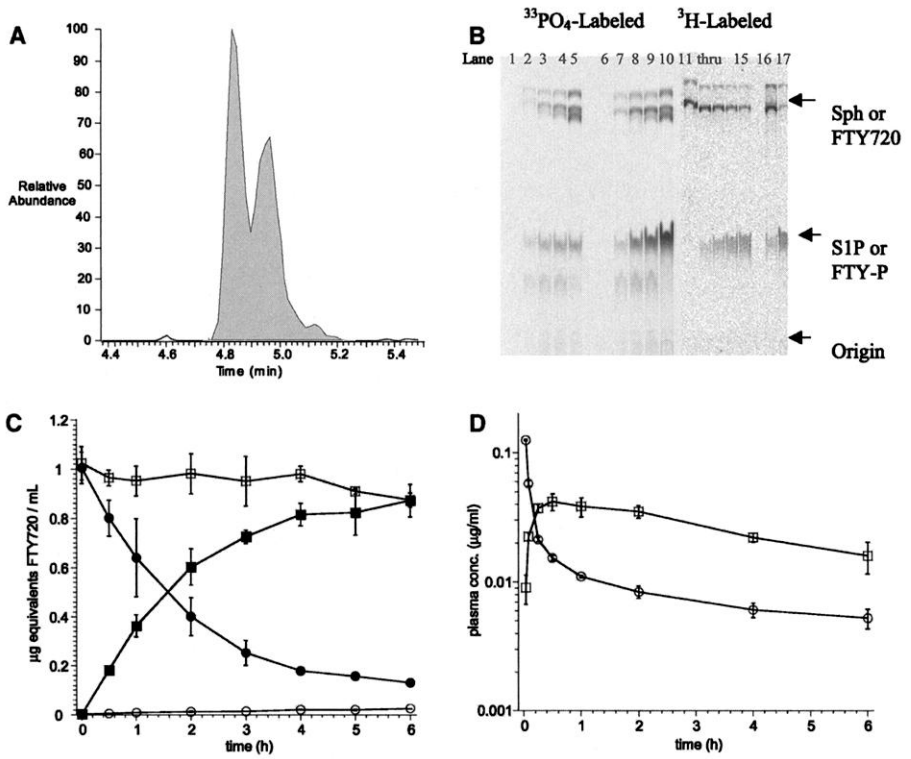


**Fig. 2.** Metabolism of FTY720 analyzed by LCMS. (**A**) FTY720 and a +80d adduct were found in mouse plasma after IV dosing with FTY720. (**B**) Phosphorimager thin-layer chromatography scan showed incorporation of $^{33}PO_4$ in FTY720 by incubation in whole rat blood: vehicle (lanes 1 to 5) and 25 µM FTY720 (lanes 6 to 10) at 0, 0.5, 2, 4, or 18 hours; rat blood with $^3$H-FTY720 at 0, 1, 2, 4, or 18 hours (lanes 11 to 15) or $^3$H-sphingosine at 30 and 60 min (lanes 16 and 17). Arrows indicate standards. (**C**) Compound A (■) was generated from FTY720 (●) by in vitro incubation of rat blood. Synthetic Compound A (□) was not converted to FTY720 (○). (**D**) FTY720 (○) was converted to Compound A (□) faster in rats (0.5 mg/kg IV) than in blood ex vivo. The steady-state ratio at 1 hour indicated dephosphorylation outside blood. See (*7*) for experimental details.

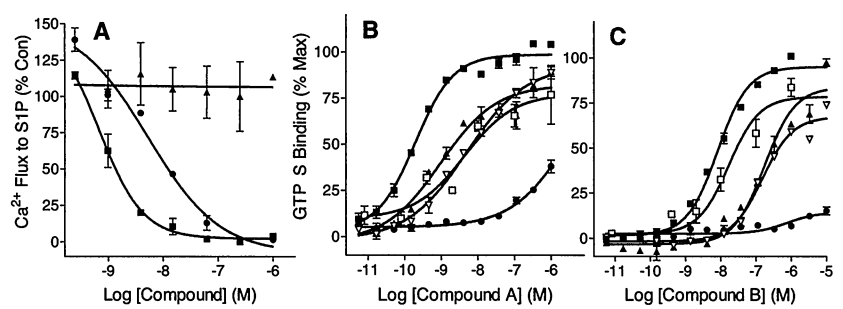


**Fig. 3.** Agonist activity of compounds (*7*). (**A**) HUVEC were pretreated with Compound A (■), S1P (●) or FTY720 (▲) for 10 min and $Ca^+$ flux in response to 200 nM sphingosine-1-phosphate was measured ($n$ = 3). (**B, C**) $^{35}$S-GTPγS binding was measured in transfected CHO cells expressing $S1P_1$ (■) $S1P_2$ (●), $S1P_3$ (△), $S1P_4$ (□), and $S1P_5$ (▲) receptors in response to Compound A (B) or Compound B (C). $EC_{50}$ values (nM) were 0.2, >1000, 4.9, 4.3 and 1.0 for Compound A, and 8.2, >10,000, 151, 33, and 178 for compound B on $S1P_1$, $S1P_2$, $S1P_3$, $S1P_4$, and $S1P_5$, respectively ($n$ = 3). See (*7*) for experimental details.

pressing each of the five S1P-binding receptors (Table 1). Compound A fully displaced S1P binding with picomolar inhibitory concentration 50% ($IC_{50}$) values on $S1P_1$ and $S1P_5$, and low nanomolar $IC_{50}$ values on $S1P_3$ and $S1P_4$. Compound A had a 20-fold higher affinity on $S1P_4$ ($IC_{50}$ = 5.9 nM) than did the putative natural ligand S1P ($IC_{50}$ = 95 nM) and, in contrast to S1P, was entirely inactive on $S1P_2$. Intrinsic affinity of FTY720 on the S1P receptors was very weak, and addition of the phosphate ester (Compound A) increased affinity at least 1000-fold on all receptors except $S1P_2$.

S1P receptors activate multiple cellular responses, through pertussis toxin (PTX)–sensitive, as well as PTX-independent transduction steps (*11, 12*). Both Compound A and S1P induced a ligand-evoked calcium flux in human umbilical vein endothelial cells (HUVEC) that express $S1P_1$ and $S1P_3$ with effective concentration 50% maximal activation ($EC_{50}$) of 3.6 and 100 nM, respectively (*7*). Compound A and S1P induced cross-desensitization of the ligand-evoked calcium flux, suggesting the ligands activate a common receptor(s). In contrast, FTY720 did not promote $Ca^{2+}$ mobilization nor induced desensitization to Compound A or S1P in HUVEC (Fig. 3). Compound A showed full agonism in CHO cells expressing cloned S1P receptors using a ligand-evoked guanosine 5′-*O*-(3-thiotriphosphate) (GTPγS) binding assay (Fig. 3), and also inhibited forskolin-induced cyclic adenosine monophosphate (cAMP) accumulation (*7*). Although no binding of S1P could be reliably detected on human naïve T cells or murine splenocytes, extracellular acidification induced by S1P or compound A could be measured by microphysiometer (*7, 8*).

To test the activity of a pharmacological S1P agonist that, unlike Compound A, was not subject to interconversion to FTY720, the nonhydrolyzable phosphonate analog of Compound A (Compound B) was synthesized (*7*). Compound B was a full agonist with nanomolar $EC_{50}$ values in the GTPγS binding assay on all the S1P receptors except for $S1P_2$, where it was inactive (Fig. 3). Although agonist potency was less for the phosphonate than the respective phosphate ester, the potency shift varied, being greatest for $S1P_5$ (~170-fold), 30- to 40-fold higher on $S1P_1$ and $S1P_3$, and only sevenfold shifted for $S1P_4$.

The nanomolar potency retained in Compound B proved sufficient for in vivo efficacy. Intravenous administration of FTY720 (2.5 mg/kg), S1P, and Compound B (5 mg/kg) produced rapid peripheral blood lymphopenia in mice and rats, reaching a nadir by 4 hours (Fig. 4A). T cells ($CD4^+$ reduced 93%, $CD8^+$ reduced 88%) and B cells (decreased 90%) disappeared from peripheral blood (*7*), whereas myelomonocytic cell numbers remained unaltered (*14, 15*). A progressive fall in both the absolute

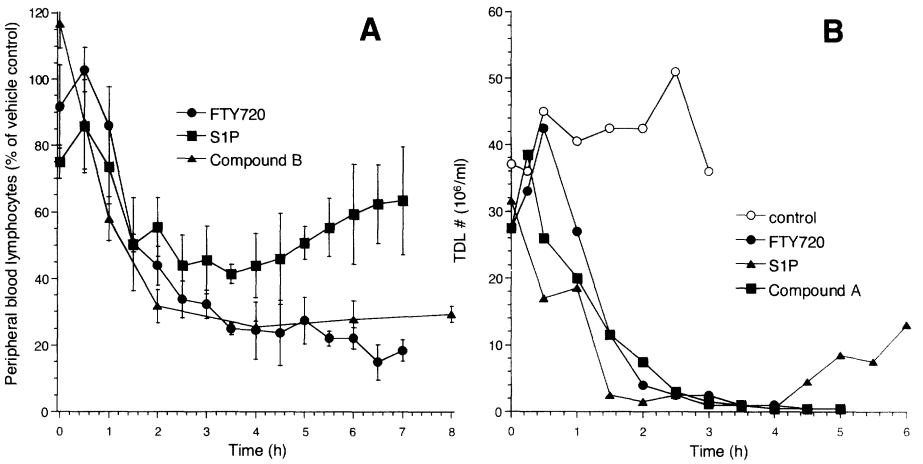


**Fig. 4.** Agonist-induced lymphopenia in blood and thoracic duct (TD) in rats. (**A**) Blood lymphocyte counts, normalized to vehicle controls, after administration of FTY720 (2.5 mg/kg oral), Compound B (5.0 mg/kg intravenous), or continuous infusion of S1P (*7*) [$n$ = 3, ± SD]. (**B**) Effect on TD lymphocyte numbers (cells/ml over 30-min collection) in cannulated rats of FTY720 (0.45 mg/kg/IV), Compound A (0.45 mg/kg/IV), S1P (infused as above), and vehicle control. S1P-induced lymphopenia was reversed upon cessation of infusion [single animals shown, representative of $n$ = 3].

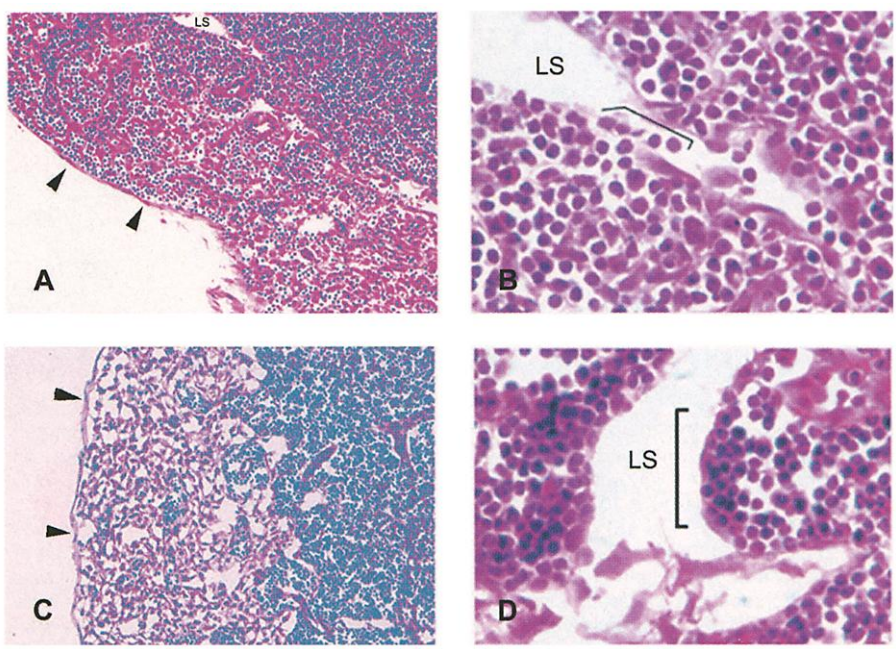


**Fig. 5.** FTY720 inhibited lymphocyte migration into murine lymphatic sinuses. (**A**) Subcapsular medullary sinuses (arrowheads) were filled with lymphocytes (vehicle control). FTY720-treated mesenteric nodes (**C**) had lymphocytes confined to B and T cell areas, with few lymphocytes in medullary and subcapsular sinuses (arrowheads). In control node (**B**), cells (bracket) appear to diapedese into lymphatic sinus (LS). LS in FTY720-treated nodes were emptied of lymphocytes (**D**), which were retained on the abluminal side of lymphatic endothelium. Original magnifications were ×200 (A and C) and ×1000 (B and D) ($n$ = 12). See (*7*) for larger view of (B) and (D).

lymphocyte count, as well as the differential count, with marked diminution of the percent blood lymphocytes occurred. Compound A had a long duration of action, reflective of its half-life and equilibrium with FTY720 (Fig. 2), whereas compound B and S1P, with shorter half-lives, showed a return to normal blood leukocyte levels within 24 hours of dosing. The relationship between the fold-potency changes in receptor $EC_{50}$s for Compound A and Compound B (Fig. 3) was confirmed in a 3-hour murine lymphopenia assay. This assay, designed to be relatively independent of pharmacokinetic differences, showed lymphopenia that correlated with intrinsic receptor potency. Under these conditions, the respective effective dose 50% reductions ($ED_{50}$s) for lymphopenia were 0.15 mg/kg for Compound A and 2.35 mg/kg for Compound B. This 15-fold shift tracked well with receptor potency and support-

**Table 1.** Binding affinities (nM) to S1P receptors.

| | $S1P_1$ | $S1P_2$ | $S1P_3$ | $S1P_4$ | $S1P_5$ |
|---|---|---|---|---|---|
| S1P | 0.47 ± 0.34 | 0.31 ± 0.02 | 0.17 ± 0.05 | 95 ± 25 | 0.61 ± 0.39 |
| Compound A | 0.21 ± 0.17 | >10,000 | 5.0 ± 2.7 | 5.9 ± 2.3 | 0.59 ± 0.27 |
| FTY720 | 300 ± 51 | >10,000 | >10,000 | >5000 | 2623 ± 317 |

$IC_{50}$ measurements determined by competition of $S1^{33}P$ binding to membranes prepared from stably transfected CHO cells expressing the indicated S1P receptor (*7*).

ed specific S1P receptor agonism rather than off-target effects. The correlation between phosphorylation and induction of lymphopenia is supported by studies on structural analogs of FTY720, in which the *R* isomer of 2-amino-4-(4-heptyloxyphenyl)-2-methylbutanol was reported to be active in a T cell depletion assay and immunosuppressive in a lymph node gain model in rats, while the *S* isomer was inactive (*16*). We synthesized the enantiomers and found that the active species was readily phosphorylated by rat blood (4.58-fold better than FTY720) and was fully efficacious at depleting lymphocytes in mice at 0.2 mg/kg, whereas the other enantiomer showed only trace phosphorylation in rat blood and was inactive at 1 mg/kg (*8*).

Quantitation of lymphocytes in thoracic duct lymph (TDL) from cannulated rats (Fig. 4B) showed that decreases in peripheral blood lymphocytes induced by S1P or Compound A were temporally associated with, or were slightly preceded by, a rapid decline in thoracic duct lymphocytes, as was seen for FTY720 (*15*). The duration of TDL lymphopenia was longer for the synthetic compounds than for S1P, correlating with compound levels in both blood and lymph (*8*). S1P, delivered by continuous infusion to avoid adverse cardiovascular effects, induced both blood lymphopenia and depletion of lymphocytes from TDL.

FTY720 has been shown to sequester cells in lymph node and not spleen (*14*). Our data in mouse and rat with Compound B show that the same pattern of sequestration was achieved with nonhydrolyzable phosphonate derivatives (*7*). Lymphocyte sequestration induced by S1P receptor agonists was observed histologically within 3 hours after a single dose. Mesenteric nodes showed disappearance of lymphocytes from subcapsular and medullary sinuses, with the logjamming of lymphocytes on the abluminal side of sinus lining endothelium (Fig. 5).

Lipid receptors may have a broad role in regulating immune responses. Although deletion of the G protein–coupled receptor for lysophosphatidylcholine (G2A) altered lymphoid organ structure and caused autoimmunity (*17*), pharmacological agonism of S1P receptors shown here causes immunosuppression. The precise role of individual S1P receptors and the hierarchy of their contributions to lymphocyte sequestration in SLO remain to be clarified, because S1P receptors are expressed on both endothelium and lymphocytes. S1P alters junctional properties of endothelium (*18, 19*). The role of the S1P receptor is separable from CCR7-dependent events because the sequestration of lymphocytes still occurred in the CCR7-deletant mice upon FTY720 treatment as shown by Henning *et al.* (*20*).

Regulation of lymphocyte trafficking through lymph node may be a physiological function of S1P, a lysosphingolipid implicated in regulating cardiac (*21, 22*) and pressor functions (*23*). Exposure to free S1P is regulated by protein and lipid binding factors in blood (*24*) and by phosphatase activities (*25*), that limit systemic side effects of S1P exposure. Regulation of blood lymphocyte numbers by systemic S1P receptor agonism may thus allow clinically useful immunosuppression through lymphocyte sequestration.

### References and Notes


1. J. L. Gowans, *Immunol. Today* **17**, 288 (1996).
2. E. C. Butcher, M. Williams, K. Youngman, L. Rott, M. Briskin, *Adv. Immunol.* **72**, 209 (1999).
3. K. M. Ansel, J. G. Cyster, *Curr. Opin. Immunol.* **13**, 172 (2001).
4. V. Brinkmann, D. D. Pinschewer, L. Feng, S. Chen, *Transplantation* **72**, 764 (2001).
5. V. Brinkmann, D. Pinschewer, K. Chiba, L. Feng, *Trends Pharmacol. Sci.* **21**, 49 (2000).
6. H. H. Neumayer *et al.*, *Transplantation* **67**, S204 (1999).
7. Supplemental material is available on *Science* Online at www.sciencemag.org/cgi/content/full/1070238/DC1.
8. S. Mandala, J. Bergstrom, R. Hajdu, data not shown.
9. J. K. Chen, W. S. Lane, S. L. Schreiber, *Chem. Biol.* **6**, 221 (1999)
10. M. H. Graeler, G. Bernhardt, M. Lipp, *Curr. Top. Microbiol. Immunol.* **246**, 131 (1999).
11. T. Hla, M.-J. Lee, N. Ancellin, J. H. Paik, M. J. Kluk, *Science* **294**, 1875 (2001).
12. N. Fukushima, I. Ishii, J. J. A. Contos, J. A. Weiner, J. Chun, *Annu. Rev. Pharmacol. Toxicol.* **41**, 507 (2001).
13. I. Ishi *et al.*, *J. Biol. Chem.* **276**, 33697 (2001).
14. Z. J. Luo, T. Tanaka, F. Kimura, M. Miyasaka, *Immunopharmacology* **41**, 199 (1999).
15. K. Chiba *et al.*, *J. Immunol.* **160**, 5037 (1998).
16. M. Kiuchi *et al.*, *J. Med. Chem.* **43**, 2946 (2000).
17. J. H. Kabarowski, K. Zhu, L. Q. Le, O. N. Witte, Y. Xu, *Science* **293**, 702 (2001).
18. M.-J. Lee *et al.*, *Cell* **99**, 301 (1999).
19. J. G. N. Garcia *et al.*, *J. Clin. Invest.* **108**, 689 (2001).
20. G. Henning *et al.*, *J. Exp. Med.* **194**, 1875 (2001).
21. K. Liliom *et al.*, *Biochem. J.* **355**, 189 (2001).
22. A. Sugiyama, Y. Yatomi, Y. Ozaki, K. Hashimoto, *Cardiovasc. Res.* **46**, 119 (2000).
23. A. Sugiyama, N. N. Aye, Y. Yatomi, Y. Ozaki, K. Hashimoto, *Jpn. J. Pharmacol.* **82**, 338 (2000).
24. N. Murata *et al.*, *Biochem. J.* **352**, 809 (2000).
25. S. M. Mandala *et al.*, *Proc. Natl. Acad. Sci. U.S.A.* **97**, 7859 (2000).


26. Acknowledgments are presented in (*7*).

25 January 2002; accepted 8 March 2002
Published online 28 March 2002;
10.1126/science.1070238
Include this information when citing this paper.


# Regulation of Mitochondrial Biogenesis in Skeletal Muscle by CaMK


**Hai Wu,[1] Shane B. Kanatous,[1] Frederick A. Thurmond,[1] Teresa Gallardo,[1] Eiji Isotani,[2] Rhonda Bassel-Duby,[1] R. Sanders Williams[3]***



**Endurance exercise training promotes mitochondrial biogenesis in skeletal muscle and enhances muscle oxidative capacity, but the signaling mechanisms involved are poorly understood. To investigate this adaptive process, we generated transgenic mice that selectively express in skeletal muscle a constitutively active form of calcium/calmodulin–dependent protein kinase IV (CaMKIV*). Skeletal muscles from these mice showed augmented mitochondrial DNA replication and mitochondrial biogenesis, up-regulation of mitochondrial enzymes involved in fatty acid metabolism and electron transport, and reduced susceptibility to fatigue during repetitive contractions. CaMK induced expression of peroxisome proliferator-activated receptor γ coactivator 1 (PGC-1), a master regulator of mitochondrial biogenesis in vivo, and activated the PGC-1 gene promoter in cultured myocytes. Thus, a calcium-regulated signaling pathway controls mitochondrial biogenesis in mammalian cells.**


The oxidative capacity of specialized myofibers in mammalian skeletal muscles can vary over an order of magnitude, thereby matching metabolic capabilities to different physiologic demands (*1*). The maximum catalytic capacity of mitochondrial enzymes involved in the tricarboxylic